Carbon Nanotube Membranes for Salt Rejection in Water Purification

Caitlyn Brahim

Abstract

Worldwide, about 700 million people have no access to clean water or sanitation. In 10 years, this number is expected to expand to 1.8 billion, or roughly one-fourth of the global population. To address this growing crisis, scientists have developed high performance synthetic membranes as a viable means of water purification. The development of these advanced membrane technologies with controlled and novel pore architectures is important for the achievement of more efficient purification, as purified water standards have recently become more stringent. Present polymeric membranes are known to suffer from a trade-off between selectivity and permeability, and in some cases are also susceptible to fouling or exhibit low chemical resistance. Membranes based on carbon nanotubes (CNTs) may provide a possible solution to overcome some of these shortcomings. This will be presented through free-standing CNT membranes, which were fabricated at various thickness and evaluated for salt rejection performance. Commercial soy-sauce was used as a model salt system, in a diffusion cell with the CNT membranes, to investigate the salt diffusion properties. In addition to free-standing CNT membranes, a commercial Millipore membrane was coated with CNT and evaluated for its salt rejection performance against the standard Millipore microfiltration membrane. The architecture of commercial Millipore membranes is analogous to the thin-film composite membranes used in reverse osmosis (RO) filtration, where a thin separation layer containing small pores is coupled to a structural layer containing large pores that acts as a structural reinforcement that supports the thin-film. The CNT membranes showed 30% greater salt rejection performance than the standard Millipore membrane. Coating CNT onto the microfiltration membrane improved its salt rejection performance by close to 50%. The results from this preliminary study illustrate the potential of using CNT membranes for enhancement in water purification.

Introduction

Interestingly, while almost 70% of the earth is covered by water, only a miniscule amount, 2.5%, is freshwater. Even then, just 1% of this freshwater is easily accessible, with much of it trapped as ice. The remaining 97.5% of the earth's water is either seawater or brackish – having less salinity than seawater but more than freshwater – therefore making it undrinkable. Along with this limited natural availability, freshwater in many regions around the world is also in decline, and recent scientific projections indicate that freshwater availability is likely to continue to decrease globally. Even as accessibility to potable water decreases, the number of people without access to improved water sources is expected to increase, given the Center for Disease Control and Prevention's (CDC) estimates that, as of 2016, 780 million people have no access. Improved water sources are designed to provide clean, drinking water for human consumption, and include piped household water connections, public standpipes, protected springs and dug wells, boreholes, and rainwater collection. According to the World Health Organization (WHO), clean water is water that has less than the allowed concentrations of dissolved matter – which varies depending on the nature of the constituent. Salted or polluted water contains suspended

particulate matter such as dust, algae, bacteria, viruses, and silt, along with various organic matter such as solvents, pesticides, and herbicides, as well as salt ions and heavy metals above the recommended concentrations. Salting and contamination of fresh water supplies therefore reiterates the necessity for increased accessibility to clean water as well as the development of more efficient water treatment technologies.

Membranes have been demonstrated to be reliable devices for decontaminating water. Various membrane types have been commercialized for application in water purification, including nanofiltration (NF) membranes with pores of ~ 2 – 3 nm for partial removal of heavy salts and large organic molecules, ultrafiltration (UF) membranes which have larger pores in the range of 10 – 100 nm, microfiltration (MF) membranes with pore diameters up to 1 μm, and reverse osmosis (RO) membranes with pores typically < 1 nm for removal of metal ions and aqueous salts. The RO membrane is considered the most promising for brackish water and seawater desalination. Typical polymeric material used in RO membranes is polyamide, which is nonporous and uses dynamic pressure for salt rejection. One crucial drawback with RO membranes, however, is that very high pressures are required to force water through them – a costly process that societies already lacking in water accessibility cannot afford. In addition, the polymeric membranes tend to be prone to corruption on their surfaces by organic impurities, and suffer from chlorine degradation during extensive desalination processing. Consequently, the development of advanced membrane technologies with novel pore architectures is important for the achievement of more efficient and cost effective purification. Equally important, such new membrane technologies must also have the potential to be translatable to the non-industrialized world. New membrane technologies based on carbon nanotubes (CNTs) may offer such potential. Due to their large specific surface area, high mechanical strength, excellent chemical inertness and outstanding water-transport property, CNTs have received widespread interest in fabrication of novel composite membranes for diverse water treatment applications.

Carbon nanotubes can be conceptually visualized as single or multiple sheets of graphene rolled into seamless cylinders with nanometer diameters (Figure 1). The former configuration results in a single wall carbon nanotube (SWCNT), while the rolling of multiple graphene sheets into concentric cylinders yields a multi wall carbon nanotube (MWCNT). CNTs exhibit remarkable electrical and thermal conductivity, and are one of the strongest fibers known ((O'Connell, M.J. Carbon Nanotubes: Properties and Applications; Taylor & Francis Group: Boca Raton, FL, USA, 2006; Dresselhaus, M.S.; Dresselhaus, G.; Avouris, Ph. Carbon Nanotubes: Synthesis, Structure, Properties,and Applications; Springer: Berlin, Germany, 2001)). These properties, combined with their nanoscale dimensions, have led to their widespread investigation for a wide range of applications ((Baughman, R.H.; Zakhidov, A.A.; De Heer, W.A. Carbon Nanotubes-the Route toward Applications. Science 2002, 297, 787–792)). The non-defective carbon atoms in the CNT structure are sp2 hybridized, and consequently van der Waals forces across the walls of individual tubes cause the material to comprehensively associate with other nanotubes. The result is a heavily bundled CNT material, which must be de-bundled into small clusters, or better still, individual nanotubes, to make use of many of their attractive properties. The de-bundling process often requires the use of appropriate dispersion solutions, including various solvents and surfactant to prevent the CNT clusters from re-agglomerating into larger bundles.

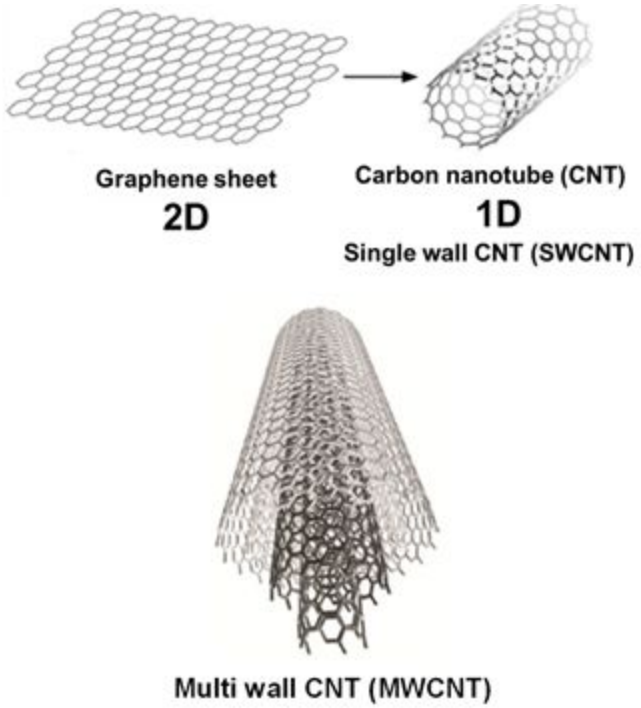

Figure 1. Schematic illustration of the relationship between a graphene sheet and carbon nanotube (CNT) structures; starting from 2-dimensional (2D) graphene sheet.

CNT in the form of Bucky-paper produced by vacuum filtration of a dilute CNT dispersion was evaluated for water purification by membrane distillation ((Sears et al. Recent developments in carbon nanotube membranes for water purification and gas separation. Materials 2010, 3, 127-149)). This technique is an alternative to reverse osmosis and other desalination techniques, particularly when the concentration of solutes is high ((Lawson, K.W.; Lloyd, D.R. Membrane Distillation. *J. Membr. Sci.* 1997, 124, 1–25)). The inherent hydrophobicity of the nanotubes (D.I. water contact angle ~113) and high Bucky-paper porosity (~90%) lend them to this application. The study demonstrated quite attractive water vapor permeabilities of up to 3.3 × 10-12 kg/m sPa on a small scale rig ((Dumée, L.F.; Sears, K.; Schütz, J.; Finn, N.; Huynh, C.; Hawkins, S.; Duke, M.; Gray, S. Characterisation and Evaluation of Carbon Nanotube Bucky-paper Membranes for Direct Contact Membrane Distillation. *J. Membr. Sci.* 2010, 351, 36-43)). However, cracking of the Bucky-papers with time was a problem as salt water penetrated into the relatively large cracks and breached the structural integrity of the CNT Bucky-paper membrane.

The cured and dried CNT membranes were peeled from the support substrate, and the free-standing CNT membranes were evaluated in a diffusion cell for salt rejection performance. The performances of the various CNT membranes were benchmarked against three classes of commercial filtration membranes – a reverse osmosis (RO) membrane, ultrafiltration (UF) membranes, and a microfiltration (MF) membrane.

Materials and Methods

CNT suspension preparation

Commercial-grade single-walled carbon nanotubes (Tuball™; OCSiAl, Columbus, Ohio) with typical impurity levels ranging from 15 to 25 wt% were used in this study. The CNT powder was subsequently dispersed in isopropyl alcohol (IPA) by high shear processing without the inclusion of a surfactant. A concentration of 8 mg of CNT per 1 mL of IPA solvent was used to prepare the CNT suspension. The resulting CNT suspension had a measured viscosity of 100,000 cP at shear rate of 0.1 s-1, and was sufficiently viscous for coating fabrication. The absence of surfactant from the CNT suspension means that no further washing treatment of the final produced CNT coatings was necessary.

CNT coating fabrication

Two techniques were used for making CNT coatings from the CNT suspension. In one method, a slot-die dispenser of fixed aperture was used to dispense CNT suspension through a coating fixture directly onto Al foil substrate (All Foils Inc., Strongsville, Ohio) positioned over a movable stage. By controlling the stage speed, CNT wet coating strips were produced along the Al foil substrate, which were thermally cured by forced evaporation of IPA solvent. Care was taken to promote removal of the IPA solvent from the CNT coating strips at a slow enough rate without causing formation of blisters or bubbles in the dried CNT coatings. The resulting coatings were peeled off of the Al foil substrate. Five repeat CNT coatings were produced in this manner (Figure 2A).

A second method was used for CNT coating fabrication whereby the slot-die coater was replaced with an adjustable knife-blade coater. In this technique, a fixed volume of CNT suspension was dispensed onto the Al foil inside a knife fixture, and the knife blade moved across the dispensed CNT suspension via the movable stage to create CNT wet coatings on the Al foil. By adjusting the knife gap, CNT coatings of varying thickness were produced. The knife-gap was adjusted to five different settings: 1.0 mm, 1.5 mm, 2.0 mm, 2.5 mm, and 3.0 mm, which resulted in the fabrication of CNT coatings of five different thicknesses after heat gun curing (Figure 2B).

In addition to pristine CNT coatings, composite CNT coatings were fabricated by the knife-coating technique by addition of high surface area activated carbon (AC, YP-80 Kuraray, Japan) to the CNT formulation. Two such composite CNT-AC coatings were fabricated, one coating containing 5 wt% AC and the second coating containing 50 wt% AC.

The CNT conformal coatings produced from both methods above were fabricated without any cracks or fractures in the coatings, and readily delaminated from the underlying Al foil substrate to yield free-standing CNT strips, which we call CNT wafers. Each CNT wafer was inspected for pinhole defects prior to evaluation in water purification testing. Regions of CNT wafers that were absent of any pinholes were cut and used as membranes in diffusion experiments.

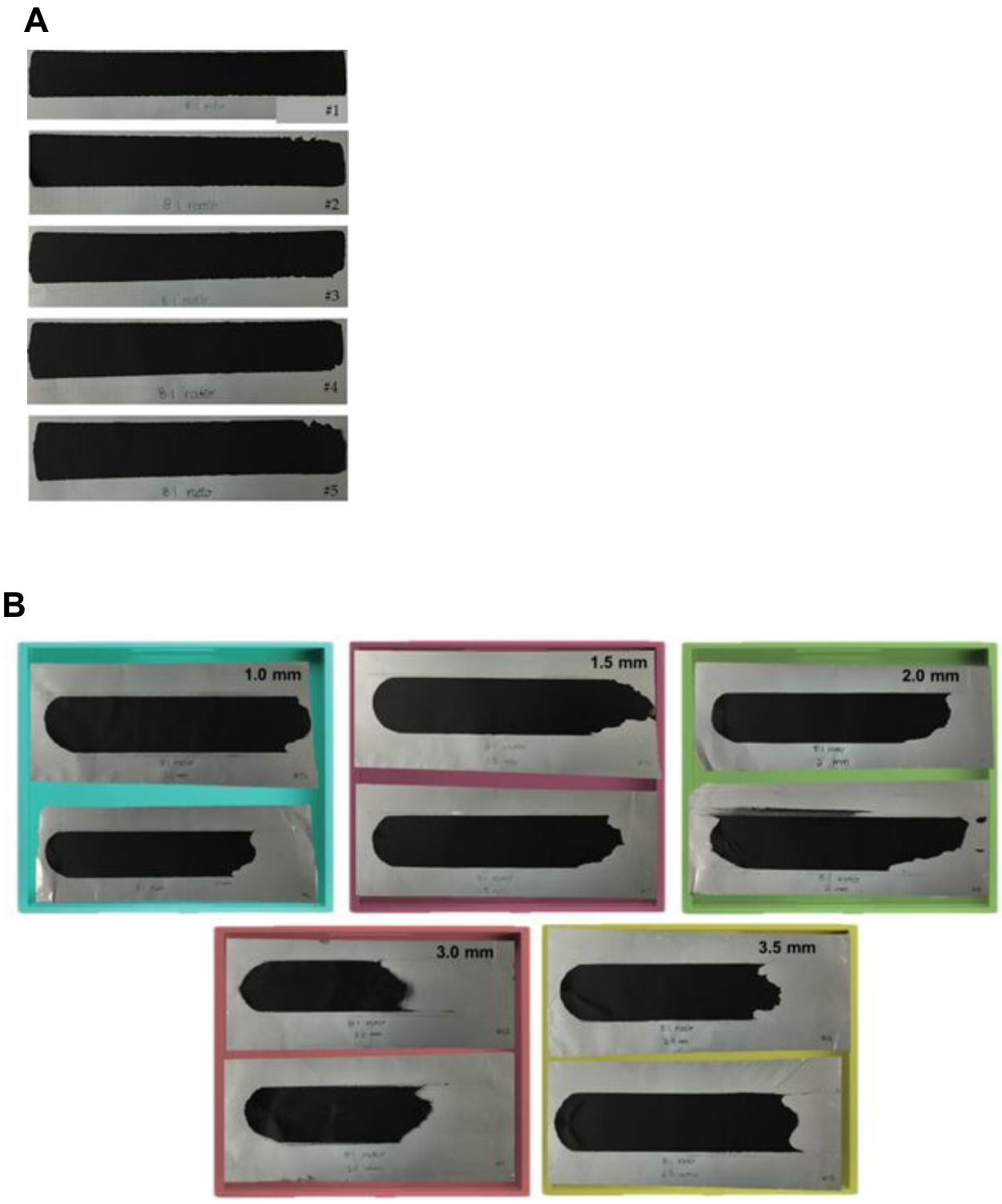

Figure 2.A) CNT coatings on foil substrates fabricated by slot-die coating from CNT-IPA dispersion (8 mg/mL), B) CNT coatings of various thicknesses on foil substrates fabricated by knife coating using different gap settings from CNT-IPA dispersion (8 mg/mL).

Membrane filtration testing

Cut portions of CNT wafers such as that shown in Figure 3A, or CNT-coated over a commercial membrane such as shown in Figure 3B, were evaluated for diffusion performance. A commercial Side-Bi-Side diffusion cell (PermeGear Inc., PA, USA) shown in Figure 4A was used for all diffusion tests. The cut portion of CNT wafer was inserted between the two halves of the membrane diffusion cell of 5 mL capacity on each side. The entire assembly was held in place using adjustable screw clamps.

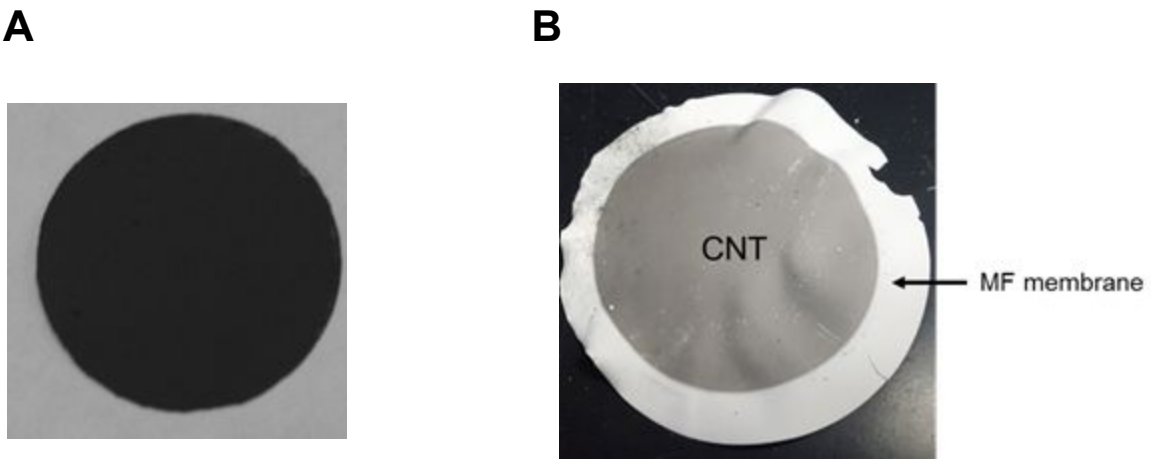

Figure 3. A) Free standing CNT membrane punched from CNT coatings; B) CNT-coated onto commercial MF membrane.

As a model salt system, soy sauce was added to one of the compartments of the diffusion cell, while deionized water was periodically placed into the second compartment. Both compartments had their contents stirred. Figure 4B shows the fully assembled diffusion cell with CNT membrane positioned between the half cells. Aliquots of the deionized water were removed periodically over time and the resulting water conductivity, as a function of diffused salt concentration, was measured using a conductivity meter and reported in units of S/cm. For benchmarking the salt rejection properties of the CNT wafers, five commercial membranes were also evaluated in the diffusion cell – three ultrafiltration membranes PVDF (Synder flat sheet membrane), TFC, and composite PA, (GE Osmonics flat sheet membrane), one reverse osmosis (RO) membrane (Dow Filmtec flat sheet membrane), and one microfiltration membrane from Millipore. Figure 4C shows the fully assembled diffusion cell with a commercial membrane positioned between the half cells.

A

B

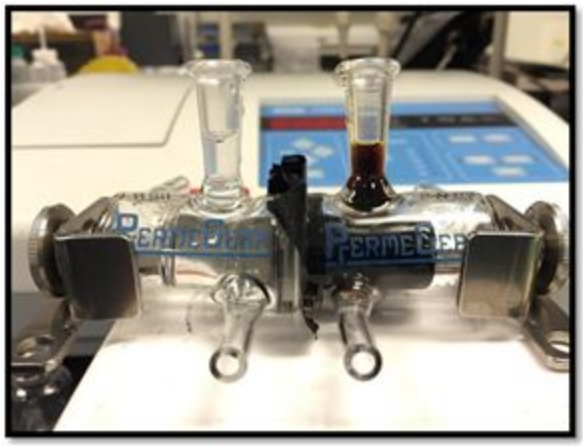

C

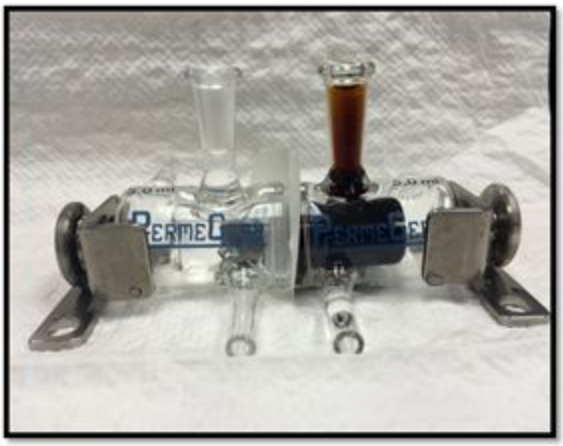

Figure 4. Apparatus used for salt rejection testing. A) Two halves of diffusion cell with clamp, B) fully assembled diffusion half-cells with stir bars in each half and CNT membrane positioned

between the two half-cells, and C) a commercial membrane inserted between two half-cells. Soy sauce was introduced into the right half-cell compartment as a model salt.

Results and Discussion

CNT wafer characterization

To capture some important physical properties of the fabricated CNT wafers such as thickness and microstructure composition, probe measurements and microscopy analyses were performed on the various CNT wafers. Due to the high aspect ratio (length to diameter ratio of > 10,000) of the CNTs and the strong van der Waals forces, the dispersed bundles in suspension readily self-associate upon removal of the dispersing solvent to form cohesive monolith networks of CNT wafers. Hence, unlike activated carbon materials, no binder is necessary in the CNT formulation to promote or enable coating formation.

Thickness

The CNT wafer thickness was measured by direct probe contact across the surface of each wafer and the measurements were averaged to calculate wafer thickness. Table 1 shows the measured thickness values (six for each wafer) and the calculated average CNT wafer thicknesses. Also included are the measured and average thickness values for commercial water filtration membranes evaluated in this study.

Thickness Measurement (mm)										
Sample ID	Coating Type	1	2	3	4	5	6	Average	Std dev	RSD (%)
#1	Slot-die	24.7	23.8	18.0	26.4	28.7	15.7	22.9	5.0	21.9
#2	Slot-die	30.0	23.1	22.4	23.9	30.0	23.2	25.4	3.6	14.0
#3	Slot-die	36.4	14.3	14.4	17.3	9.1	16.6	18.0	9.5	52.5
#4	Slot-die	25.8	17.3	16.3	17.7	17.3	18.9	18.9	3.5	18.5
#5	Slot-die	16.7	9.6	18.0	19.6	28.0	24.7	19.4	6.4	33.1

1.0 mm A	Knife gap	18.7	25.7	33.7	24.8	39.1	28.5	28.4	7.2	25.2
1.0 mm B	Knife gap	22.4	31.0	25.3	23.2	19.5	33.2	25.8	5.3	20.5
1.5 mm A	Knife gap	30.7	28.7	26.7	27.2	22.7	21.2	26.2	3.6	13.8
1.5 mm B	Knife gap	27.2	30.2	19.7	26.0	34.8	29.7	27.9	5.0	18.1
2.0 mm A	Knife gap	33.5	23.2	28.5	28.5	25.7	21.7	26.9	4.3	15.9
2.0 mm B	Knife gap	22.8	27.1	33.3	21.0	25.3	28.1	26.3	4.3	16.5
2.5 mm A	Knife gap	27.5	37.1	46.4	33.0	53.3	51.0	41.4	10.4	25.1
2.5 mm B	Knife gap	34.6	33.5	42.5	38.1	44.3	36.0	38.2	4.4	11.5
3.0 mm A	Knife gap	47.1	62.4	45.6	37.9	48.7	47.1	48.1	8.0	16.5
3.0 mm B	Knife gap	51.0	52.9	48.5	66.6	49.7	57.9	54.4	6.8	12.5
PVDF	Membrane	178.8	178.6	173.5	174.8	181.0	178.7	177.6	2.8	1.6
TFC	Membrane	117.3	126.3	121.9	117.9	120.8	123.8	121.3	3.4	2.8
RO	Membrane	131.4	130.7	135.2	139.2	129.5	133.8	133.3	3.6	2.7
Composite PA	Membrane	141.9	139.5	137.3	132.6	236.1	135.6	153.8	40.4	26.3
Millipore	Membrane	142.8	138.5	129.8	129.2	130.3	135.4	134.3	5.5	4.1

Table 1. Measured and average thickness values for fabricated CNT wafers and commercial water filtration membranes.

From Table 1 it is seen that the average CNT coating thickness for wafers fabricated by the slot-die coater was 20 μm. These were thinner than CNT wafers produced by the knife-coater, which varied according to the set knife gap. Figure 5A captures this variation. CNT wafers fabricated using knife gap settings of 1.0 – 2.0 mm had similar coating thicknesses close to 27 μm. Increasing the gap size to 2.5 mm resulted in the fabrication of CNT wafers of average thickness 40 μm. The thickest CNT wafers in the study had an average thickness of 50 μm using the largest knife gap setting of 3.0 mm. As shown in the comparative plot of average membrane thickness in Figure 5B, all fabricated CNT wafers were substantially thinner than commercial water filtration membranes, which had average thickness > 100 μm. Among these, the PVDF membrane was the thickest commercial membrane investigated in the study with a thickness approaching 180 μm. The other commercial membranes had an average thickness closer to 130 μm.

A

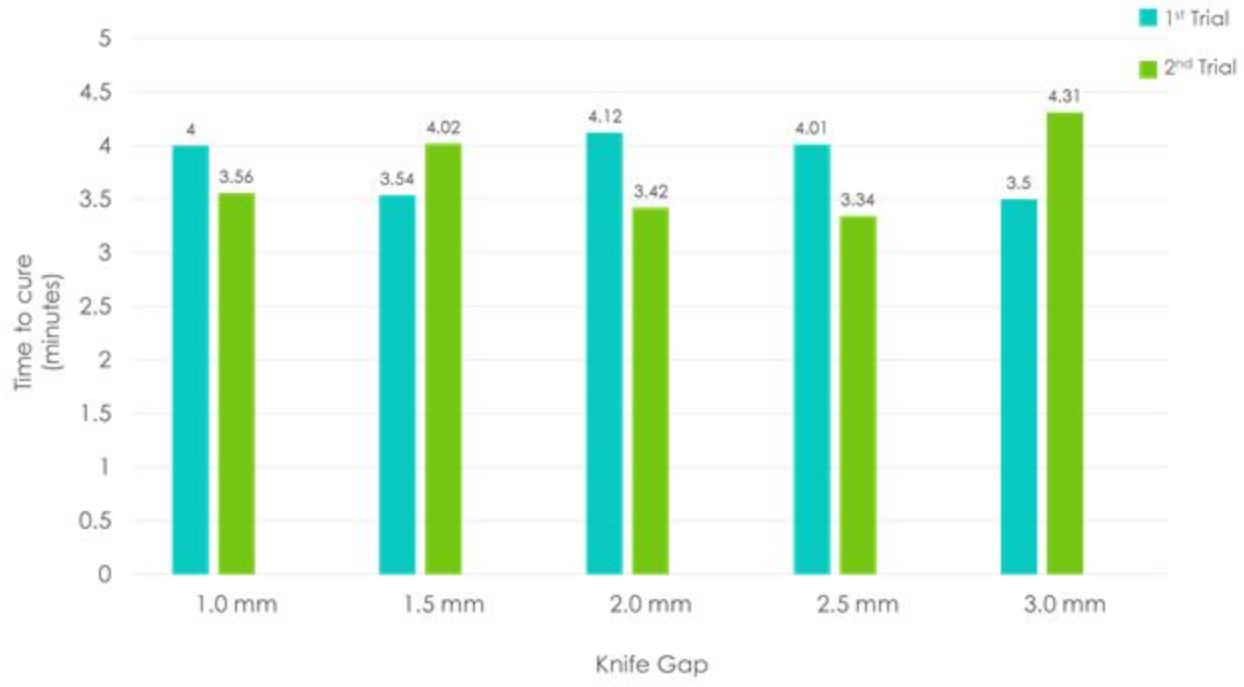

B

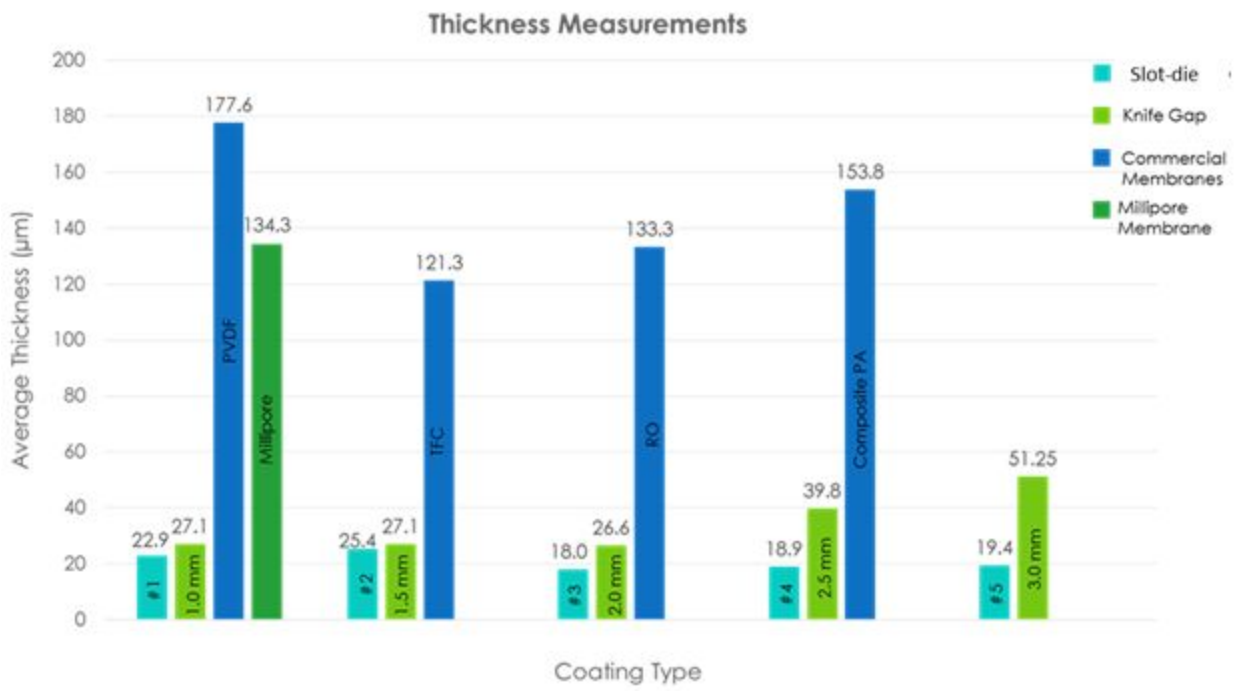

Figure 5. A) Variation in CNT wafer thickness produced by knife coating using different gap settings, B) Variation in CNT wafer thickness produced by slot-die coating and knife coating. For reference, the average thickness of the commercial membranes evaluated in this study are included.

Membrane microstructure

Optical micrographs of the various CNT wafers are shown in Figure 6A and compared with the commercial filtration membranes (Figure 6B). For the CNT wafers, the images show several CNT bundles at the stated magnification. The composition of the CNT wafers appears significantly different from the commercial membranes. The optical microscope does not have sufficient magnification to resolve individual nanotubes within the CNT bundles that compose the wafers. To achieve this higher, more detailed microscopic resolution, a scanning electron microscope was used, which permitted imaging at magnifications > 50,000. A scanning electron microscope was used to provide higher microscopic resolution. At this higher magnification, resolution down to few CNT nanotube bundles in the wafers is afforded as shown in Figure 6C. Cross sectional imaging was also performed on cut CNT wafers, from which another estimation of wafer thickness can be performed. All CNT wafer images confirm a random entanglement of CNT bundles throughout the porous macroscopic wafer structure.

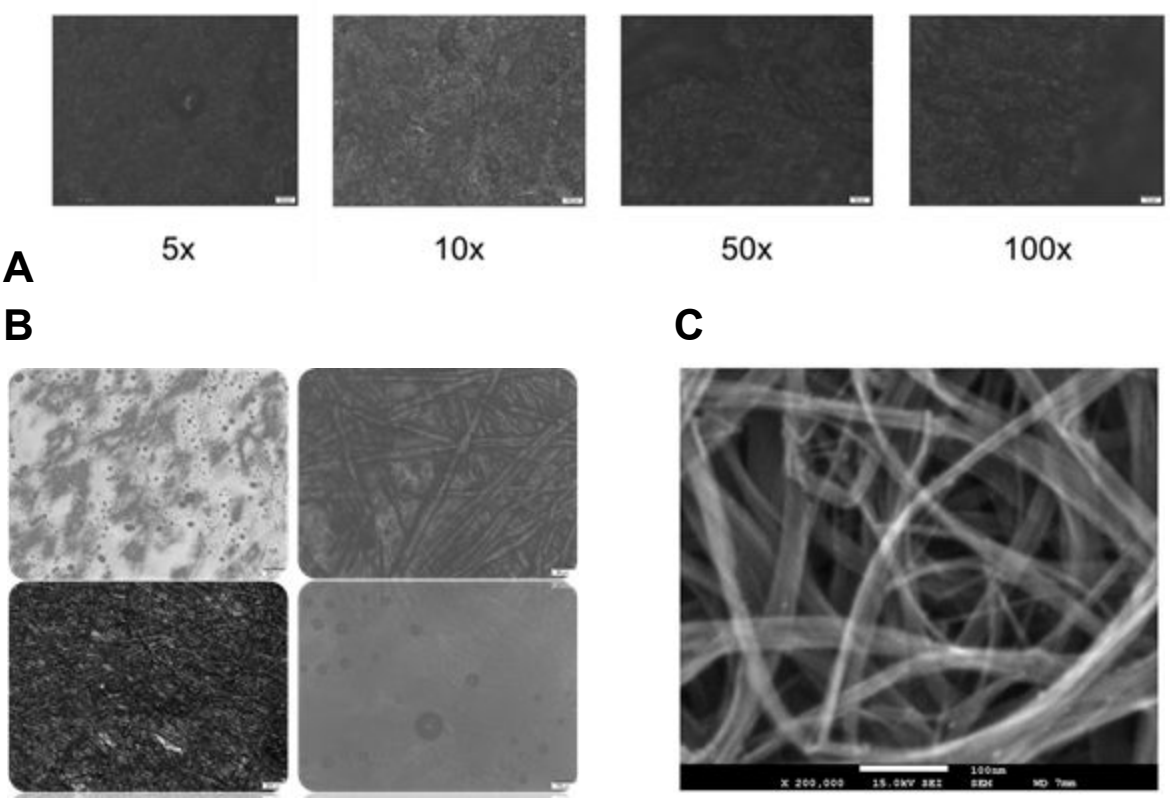

Figure 6. Optical micrographs of A) CNT membranes and B) commercial filtration membranes, C) High resolution SEM image of CNT membranes showing random orientation of CNT bundles.

Diffusion cell performance

To evaluate the efficacy of each membrane type for salt rejection, a commercial diffusion cell for small volumes was setup as shown in Figure 4. The initial salt concentration at time t0 in the diffusion cell compartment containing the soy sauce was quantified via ionic conductivity measurement and gave an average conductivity value of around 36,000 µS/cm. The effectiveness of each membrane in the cell to screen the diffusion of salt across the compartments was evaluated by measuring the diffused salt concentration as a function of time. A total of eleven membranes was evaluated, among which were the five commercial non-carbon based filtration membranes, and six CNT-based membranes. Figure 7 shows the resulting time-dependent diffusion profiles for each investigated membrane. As a baseline, the conductivity of deionized water (simulating freshwater) was measured at 38 µS/cm.

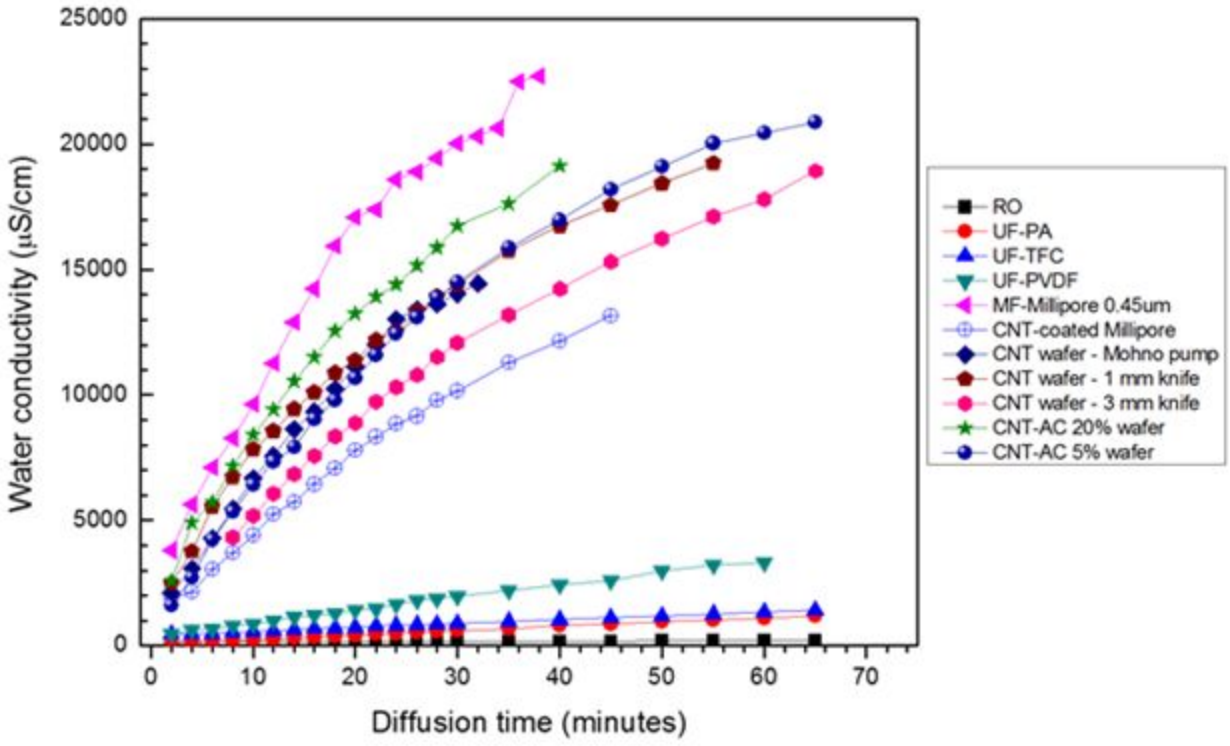

Figure 7. Time-dependent diffusion profiles for CNT membranes and commercial membranes.

Commercial membrane performance

As a group, the commercial membranes tended to have a linear diffusion profile, in contrast to the hyperbolic-shaped profile of the CNT-based membranes. The most effective screening of salt was achieved using the commercial reverse osmosis membrane (RO), which showed a very low diffused salt concentration across the membrane as evidenced by the low measured ionic conductivity value of 200 µS/cm after more than 60 minutes of salt diffusion. The three ultra-filtration (UF) membranes showed next lowest quantities of diffused salt, depending on the membrane composition. The composite polyalcohol UF membrane PA showed the lowest salt concentration (~1,200 µS/cm) after 60 minutes, followed by the thin film composite (TFC) UF membrane (1,400 µS/cm). The PVDF-based UF membrane allowed the highest salt concentration to diffuse through the compartment, resulting in a measured conductivity value of 3,300 µS/cm. The compartment using the commercial Millipore membrane showed the highest measured conductivity value of close to 23,000 µS/cm, corresponding to largest influx of diffused salt across the membrane. These results can be interpreted by the porosity of the different membranes. The RO membrane typically has pores of average size 0.1 to 1.0 nm, thus significantly limiting solvated salt diffusion, which is reflected in the corresponding very low conductivity value. The ultrafiltration membranes PA and TFC tend to have pores in the lower range of 5 – 100 nm and yield similar conductivity values. The third UF membrane composed of PVDF may have slightly larger pores closer to 100 nm, hence resulting in the larger measured

conductivity value. The Millipore membrane is a type of microfiltration membrane with pores closer to 0.45 μm. Consequently, the micron-sized porosity of this commercial membrane allows the solvated salt to diffuse through with least resistance to flow, resulting in the largest measured conductivity value.

CNT membrane performance

Representatives from the three classes of fabricated CNT membranes, slot-die coated CNT, knife-coated CNT, and composite CNT-AC membranes, were selected for evaluation as barrier membrane in the diffusion cell with the salt solution in one compartment. The resulting time-dependent salt diffusion profiles, shown in Figure 7, were all found to lie between the profiles measured for the commercial PVDF-based UF membrane and the Millipore microfiltration membrane. The porosity of similar fabricated CNT structures was previously reported to be 10 nm or greater, suggesting that the CNT membranes of the present study possess a high meso-porosity. This agrees well with the observed diffusion profile trends of the CNT membranes.

Additional trends can be discerned from the diffusion profiles of the various CNT membranes. First, the CNT membrane thickness appears to have an influence on salt rejection performance. The thickest CNT membrane of ca. 5 0 μm fabricated by knife coating with 3 mm gap showed the lowest measured salt conductivity value of 12,000 μS/cm after 30 minutes. In comparison, the slot-die coated CNT membrane and 1 mm gap knife-coated CNT membrane, both with thickness around 25 μm, showed higher salt conductivity values of around 14,000 μS/cm after 30 minutes. This pattern seems to indicate that thicker CNT membranes would be more effective in salt rejection performance. In fact, the CNT membrane thickness is significantly thinner than the commercial membranes which have average thickness > 100 μm. Second, the effect of adding high surface area activated carbon (AC) to the CNT to fabricate composite membranes was not advantageous to salt rejection performance. Both the 5 wt% and 20 wt% AC formulations showed equal or higher salt conductivity values than the pristine CNT membranes. It should be noted that all CNT membranes retained their mechanical and structural integrity after completion of the salt rejection tests, and no fractures or cracks were observed in the membranes. Further fine tuning of CNT network porosity in the free-standing membrane structures is anticipated to enhance their salt rejection performance.

Finally, the use of CNT as an overcoat layer on a commercial microfiltration membrane to enhance its salt rejection performance was explored. Briefly, the commercial Millipore membrane was coated on one side by a thin layer of CNT using vacuum filtration (Figure 3B). The CNT-coated Millipore membrane was introduced into the diffusion cell with the CNT-coated side in contact with the compartment containing the salt solution. As Figure 10 shows, the CNT coating resulted in a 50% reduction in salt diffusion across the Millipore membrane, with a measured conductivity value of 10,000 μS/cm compared to 20,000 μS/cm after 30 minutes for the bare Millipore membrane. A comparison of measured conductivity values for the CNT membranes and commercial membranes is summarized in Table 2.

Sample ID	Coating Type	Conductivity after 30 minutes (μS/cm) Deionized water side
#4	Slot-die	13,870
1.0 mm A	Knife gap	14,000
3.0 mm A	Knife gap	12,000
CNT-AC 5%	Knife gap	14,000
CNT-AC 20%	Knife gap	17,000
CNT/Millipore	Overcoat	10,000
PVDF	Membrane	2000
TFC	Membrane	900
RO	Membrane	200
Composite PA	Membrane	650
Millipore	Membrane	20,000

Table 2. Measured conductivity values for fabricated CNT wafers and commercial water filtration membranes in a diffusion cell with aqueous salt solution.

A comparative rating of the screening properties of the CNT membranes fabricated in the present study to common types of membranes is presented in Figure 8. It can be seen that the salt rejection performance of CNT membranes lies in the intersection of ultrafiltration and microfiltration membrane performance. Moreover, as this study shows, the salt rejection performance of a commercial microfiltration membrane can be significantly improved by using a CNT overcoat layer.

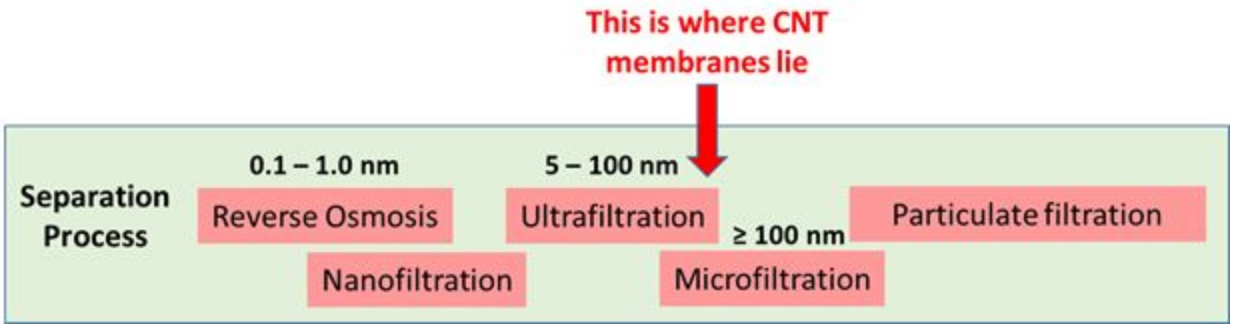

Figure 8. Comparative rating of the screening properties of the CNT membranes fabricated in the present study to common types of membranes.

Conclusion

Free standing carbon nanotube (CNT) membranes of different thicknesses were fabricated from surfactant-free dispersions via slot-die coating and knife coating processes for application in water filtration. Composite CNT-activated carbon membranes were also fabricated containing 5 wt% and 20 wt% activated carbon content. The CNT membranes were introduced into a diffusion cell with aqueous salt solution and their salt rejection performances were compared to commercial water filtration membranes. The CNT membrane performance was found to be less efficient than that of commercial ultrafiltration membranes and reverse osmosis membrane for salt rejection. However, the CNT membranes were shown to be about 30% more effective in salt rejection performance compared to a commercial microfiltration membrane. Applying a thin coating of CNT over the commercial microfiltration membrane resulted in 50% improvement in its salt rejection performance. These findings highlight the potential use of carbon nanotubes in the fabrication of composite water filtration membranes that may offer higher flux for better particulate retention or virus removal.

The use of nanomaterials such as CNTs may also afford improvement over present water desalination membranes such as thick polyamide membranes. It requires a significant amount of energy to force water through these polymer membranes for salt removal, making the process quite costly. Nano-engineering approaches to fabricating composite membranes incorporating CNTs or graphene could offer improved surface wettability with less resistance, resulting in overall more efficient water filtration and desalination technologies.

Acknowledgments

I express my deepest gratitude to Dr. Thomas Lazzara (Meissner Filtration) and Mr. Erik Indra (YTC America, Inc.) for their guidance and instruction throughout this project. I am also grateful to YTC America, Inc. for providing me with a research opportunity that allowed me to conduct this research.

References

Baughman, Ray H., et al. “Carbon Nanotubes--the Route Toward Applications.” *Science*, American Association for the Advancement of Science, 2 Aug. 2002, science.sciencemag.org/content/297/5582/787.

"Competing for Clean Water Has Led to a Crisis." *Clean Water Crisis Facts and Information*, 27 Jan. 2017, www.nationalgeographic.com/environment/freshwater/freshwater-crisis/.
Das, Rasel, et al. "Carbon Nanotube Membranes for Water Purification: A Bright Future in Water Desalination." *Desalination*, Elsevier, 24 Jan. 2014, www.sciencedirect.com/science/article/pii/S0011916413006127.
De Volder, Michael, Tawfick, Sameh, Baughman, Ray, Hart John. "Carbon nanotubes: Present and future commercial applications." *Science*, vol. 339, no. 6119, 2013, pp. 535–539.
Dresselhaus, Mildred S., et al. *Carbon Nanotubes Synthesis, Structure, Properties, and Applications*. Springer Berlin, 2014.
"Drinking-Water." *World Health Organization*, World Health Organization, 7 Feb. 2018, www.who.int/news-room/fact-sheets/detail/drinking-water.
Dumée, Ludovic F, et al. "Characterization and Evaluation of Carbon Nanotube Bucky-Paper Membranes for Direct Contact Membrane Distillation." *Journal of Membrane Science*, Elsevier, 20 Jan. 2010, www.sciencedirect.com/science/article/pii/S0376738810000347.
"Global WASH Fast Facts | Global Water, Sanitation and Hygiene | Healthy Water | CDC." *Centers for Disease Control and Prevention*, Centers for Disease Control and Prevention, 11 Apr. 2016, www.cdc.gov/healthywater/global/wash_statistics.html.
Goh, Kunli, et al. "Carbon Nanomaterials for Advancing Separation Membranes: A Strategic Perspective." *Carbon*, Pergamon, 24 Aug. 2016, www.sciencedirect.com/science/article/pii/S0008622316307321.
Goh, P.S., et al. "Carbon Nanotubes for Desalination: Performance Evaluation and Current Hurdles." *Desalination*, Elsevier, 28 Aug. 2012, www.sciencedirect.com/science/article/pii/S0011916412004237.
Kim, Jeonghwan, and Bart Van der Bruggen. "The Use of Nanoparticles in Polymeric and Ceramic Membrane Structures: Review of Manufacturing Procedures and Performance Improvement for Water Treatment." *Environmental Pollution*, Elsevier, 28 Apr. 2010, www.sciencedirect.com/science/article/pii/S0269749110001302.
Lawson, Kevin W., and Douglas R. Lloyd. "Membrane Distillation." *Journal of Membrane Science*, Elsevier, 26 Mar. 1998, www.sciencedirect.com/science/article/pii/S0376738896002360.
Lee, Kwang-Jin, and Hee-Deung Park. "Effect of Transmembrane Pressure, Linear Velocity, and Temperature on Permeate Water Flux of High-Density Vertically Aligned Carbon Nanotube Membranes." *Taylor & Francis*, 20 June 2016, www.tandfonline.com/doi/abs/10.1080/19443994.2016.1189704.
Liu, Wenbin, et al. "Global Freshwater Availability Below Normal Conditions and Population Impact Under 1.5 and 2 °C Stabilization Scenarios." *Geophysical Research Letters*, vol. 45, no. 18, 2018, pp. 9803-9813.
OConnell, Michael J. *Carbon Nanotubes: Properties and Applications*. CRC Press, 2007.
Sears, Kallista et al. "Recent Developments in Carbon Nanotube Membranes for Water Purification and Gas Separation." *Materials*, vol. 3, no. 1, 2010, pp. 127–149.